Research Article | Vol. 27, No. 10 | 13 May 2019 | OPTICS EXPRESS 14487
Optics EXPRESS

Numerical investigation of GHz repetition rate fundamentally mode-locked all-fiber lasers

YUNXIU MA,[1,2] XIUSHAN ZHU,[2,4] LUYUN YANG,[1,5] MINGHONG TONG,[2] ROBERT A. NORWOOD,[2] HUAI WEI,[3] YINGBO CHU,[1] HAIQING LI,[1] NENGLI DAI,[1] JINGGANG PENG,[1] JINYAN LI,[1] AND NASSER PEYGHAMBARIAN[2]

[1]*Wuhan National Laboratory for Optoelectronics, Huazhong University of Science and Technology, Hubei 430074, China*
[2]*College of Optical Science, the University of Arizona, Tucson, AZ 85721, USA*
[3]*Key Laboratory of All-Optical Networks and Advanced Communication Networks of Ministry of Education, Beijing Jiaotong University, Beijin, 100044, China*
[4]*xszhu@email.arizona.edu*
[5]*luyunyang@gmail.com*

Abstract: GHz repetition rate fundamentally mode-locked lasers have attracted great interest for a variety of scientific and practical applications. A passively mode-locked laser in all-fiber format has the advantages of high stability, maintenance-free operation, super compactness, and reliability. In this paper, we present numerical investigation on passive mode-locking of all-fiber lasers operating at repetition rates of 1-20 GHz. Our calculations show that the reflectivity of the output coupler, the small signal gain of the doped fiber, the total net cavity dispersion, and the modulation depth of the saturable absorber are the key parameters for producing stable fundamentally mode-locked pulses at GHz repetition rates in very short all-fiber linear cavities. The instabilities of GHz repetition rate fundamentally mode-locked all-fiber lasers with different parameters were calculated and analyzed. Compared to a regular MHz repetition rate mode-locked all-fiber laser, the pump power range for the mode-locking of a GHz repetition rate all-fiber laser is much larger due to the several orders of magnitude lower accumulated nonlinearity in the fiber cavity. The presented numerical study provides valuable guidance for the design and development of highly stable mode-locked all-fiber lasers operating at GHz repetition rates.

1. Introduction

Mode-locked laser sources capable of producing ultrashort pulses with femtosecond (fs) to picosecond (ps) durations have enormous impacts on many disciplines of science and technology. A growing number of scientific and practical applications rely on mode-locked lasers with high peak power sufficient to accomplish the tasks on an ultrashort timescale without inducing any other side effects [1]. Mode-locked lasers fundamentally operating at gigahertz (GHz) repetition rates exhibit large mode spacings and high signal-to-noise ratios, and have shown their advantages in a variety of applications including ultra-high speed communication, spectroscopy, precision optical sampling, material processing, and biology [2–13]. For instance, a GHz repetition rate mode-locked laser frequency comb allowing to access and manipulate of each individual comb line with high accuracy can be used for optical arbitrary waveform generation, high-speed analog-to-digital conversion and high-resolution spectroscopy [8]. A mode-locked laser source operating at a repetition rate greater than 10 GHz is an ideal broadband calibration standard that can be used to search the earth-like exoplanets [9–13].

GHz repetition rate mode-locked laser sources have been developed with solid state lasers [14,15], semiconductor lasers [16,17], and fiber lasers [18–34]. The repetition rate of a diode-pumped mode-locked solid-state laser can be as high as a few hundred GHz [14,15].

#360352 https://doi.org/10.1364/OE.27.014487
Journal © 2019 Received 27 Feb 2019; revised 12 Apr 2019; accepted 23 Apr 2019; published 6 May 2019

Optics EXPRESS

However, mode-locked solid-state lasers usually lack long-term stability and reliability due to their free-space configurations, which mainly limits their use in many applications. Mode-locked semiconductor lasers can be very compact and robust and have been used to generate ultrashort pulses at very high repetition rates (> 10 GHz) for fast data transmitters in optical fiber communications and all-optical signal processing. However, their pulse qualities are generally poor due to the additional satellite pulses, timing jitters, and chirped phases [23,24]. Fiber lasers having the advantages of low manufacturing and maintaining cost, excellent beam quality, and outstanding heat dissipation capability, have become excellent laser platforms for GHz repetition rate mode-locked laser sources with high reliability and good pulse quality [18–34].

A fiber laser can be mode-locked either actively with an optical modulator or passively with a saturable absorber (SA), technique of nonlinear polarization evolution, or technique of four-wave-mixing [19–22]. Fundamental mode-locking of a fiber laser with an electro-optic modulator usually operates at MHz repetition rate constrained by the cavity length [18]. Actively mode-locked pulses at GHz repetition rates can be achieved with harmonic mode-locking of a fiber laser [19]. However, the pulse width of an actively mode-locked fiber laser is usually long and the pulses usually do not have constant energies and coherent mutual phases. Moreover, actively mode-locked fiber lasers require external electronic control devices and high-speed modulators which make the laser source very complicated and expensive. Compared to actively mode-locked fiber lasers, passively mode-locked fiber lasers can generate much shorter pulses with high mutual phase coherence and even GHz repetition rate fundamentally mode-locked pulses can be obtained with very simple and compact setups. A numbers of GHz repetition rate fundamentally mode-locked fiber lasers have been achieved with centimeter or even sub-cm long gain fibers [23–34]. However, some of these lasers were developed with free-space cavities, which have not taken advantages of compactness and robustness of fiber lasers [23–28]. The mode-locked lasers developed in all-fiber configurations have shown outstanding stability and reliability [29–34]. A 12 GHz repetition rate fundamentally mode-locked all-fiber laser (FML-AFL) was demonstrated with an 8-mm long highly Er^{3+}/Yb^{3+} co-doped phosphate fiber [34]. Using a 4.75 mm highly Er^{3+}/Yb^{3+} co-doped phosphosilicate fiber, Martinez and Yamashita demonstrated an FML-AFL operating with a fundamental repetition rate as high as 19.45 GHz [32]. However, the output stability of this laser is poor due to the thermal effect of the unabsorbed pump on the saturable absorber. Nevertheless, it is still possible to develop a stable 20 GHz repetition rate FML-AFL with low noise and time-jitter using current highly doped phosphate fiber technology, where a dopant concentration of Yb^{3+} up to 12 wt. % has been achieved without concentration quenching effects [35]. GHz repetition rate pulses can also be obtained from harmonic mode-locking of a long-cavity fiber laser with a fundamental repetition rate of MHz [36–39], in which multiple pulses are formed within a round trip due to the nonlinear effects [37]. Most recently, a mode-locked fiber laser operating at the 3436^{th} harmonic of the fundamental repetition rate was developed and pulses with a repetition rate of 14.5GHz were obtained [38]. Harmonic mode-locked fiber lasers with tunable repetition rate at GHz ranges have also been achieved with four-wave mixing mechanism and different frequency multiplication techniques [19–22]. However, harmonic mode-locking of a fiber laser is usually much less stable than fundamental mode-locking and is also harder to control for practical applications [39]. Therefore, GHz repetition rate FML-AFLs are preferred for the applications mentioned above. However, compared to conventional MHz repetition rate FML-AFLs, it is more challenging to develop stable GHz repetition rate FML-AFLs because the peak power of the laser in the cavity is much lower and there is much less room for dispersion management and instability suppression in a cm-long or sub-cm-long fiber cavity. Therefore, thorough understanding of the mode-locking of cm-long or sub-cm-long fiber lasers with various parameters is very necessary for us to design and develop GHz repetition rate FML-AFLs.

Optics EXPRESS

Numerical simulation can essentially help us to understand the experimental results and provide guidelines for optimizing the design and development.

Numerical investigations on mode-locked fiber lasers have been extensively conducted by solving the nonlinear Schrödinger equation [40]. The performance of mode-locked fiber lasers with various net cavity dispersions has been numerically studied and analyzed [41–56]. These theoretical works have successfully explained most features and behaviors of MHz repetition rate mode-locked fiber lasers and provided us comprehensive understanding of nonlinear dynamics, pulse evolution, and instability of mode-locked lasers. However, these analyses and conclusions may not be applied for GHz repetition rate mode-locked AFLs in which the peak powers are much lower than those of MHz repetition rate mode-locked fiber lasers and the net cavity dispersions cannot be managed easily. Most recently, pulse instability of sub-GHz to 2 GHz repetition rate FML fiber lasers at different pump power levels was numerically studied [57]. However, the pump power is a parameter that can be easily varied and controlled even after the fiber laser is developed. The modulation depth (MD) of the saturable absorber, the total dispersion of the fiber cavity, and the reflectivity of the output coupler, in principle, are pre-manufacturing parameters that strongly influence the performance of a mode-locked fiber laser. Thus, comprehensive numerical investigation on the influence of these parameters on the performance of GHz repetition rate mode-locked AFLs is very important and helpful for the design and development of GHz repetition rate FML-AFLs with high stability and low noises. In this paper, we present our numerical studies on the GHz repetition rate FML-AFLs for key parameters including the total net cavity dispersion, the small-signal gain of the gain fiber, and the MD of saturable absorber with different values. Guidelines for the design and development of the GHz repetition rate FML-AFLs are given based on the simulation results.

2. Theoretical model

The basic configurations of GHz repetition rate mode-locked AFLs are shown in Fig. 1. Figure 1(a) is a linear cavity consisting of a chirped fiber Bragg grating (CFBG), a short piece of passive single mode fiber (SMF), a short piece of highly doped gain fiber (GF), and a saturable absorber (SA) such as semiconductor saturable absorption mirror (SESAM). The CFBG is used for the cavity net dispersion compensation and as an output coupler as well. The SA works as a mode locker and a high reflectivity cavity mirror. The total fiber cavity length corresponding to different repetition rates can be adjusted by changing the lengths of the passive SMF and gain fiber. Dielectric thin film coated on an optical fiber can be used as the output coupler when the required cavity length becomes too short to use a CFBG anymore. Figure 1(b) is a linear cavity for higher repetition rate mode-locked AFLs, where the CFBG and SMF is replaced by a dichroic coupler (DC).

Fig. 1. The configurations of (a) a GHz repetition rate mode-locked AFL in which a CFBG is used as the output coupler and (b) a GHz repetition rate mode-locked AFL in which a fiber-optic dichroic mirror is used as the output coupler.

Similar to the modeling of mode-locked fiber lasers operating at MHz repetition rates, the numerical simulation of GHz repetition rate mode-locked AFLs is carried out by solving the nonlinear Schrödinger equation with the split-step Fourier algorithm [58–60]:

Optics EXPRESS

$$\frac{\partial A}{\partial z} = -\frac{i\beta_2}{2}\frac{\partial^2 A}{\partial t^2} + i\gamma|A|^2 A + \frac{g}{2}A + \frac{g}{2\Omega^2}\frac{\partial^2 A}{\partial t^2} \tag{1}$$

where, A is the slowly varying amplitude of the pulse envelop, z is the light propagation coordinate, t is the time-delay parameter, β_2 is the second-order dispersion, γ is the $\chi^{(3)}$ nonlinearity parameter, Ω and g represent the gain bandwidth and the gain coefficient of the highly doped gain fiber, respectively, and g is written as [61]

$$g = \frac{g_0}{1 + \int |A|^2 dt / E_{sat}} \tag{2}$$

where, g_0 and E_{sat} are the small-signal gain and saturation energy of the highly doped gain fiber, respectively. Because the gain fiber length of a GHz repetition rate mode-locked AFL is comparable to the gain medium length of a solid-state laser, we assume that g_0 is constant along the gain fiber. It should be noted that both the peak power and the fiber cavity length of a GHz repetition rate fiber are at least two orders of magnitude smaller than those of a MHz repetition rate fiber laser. Therefore, the split-step Fourier method can provide enough accuracy for our simulation.

The reflectivity of the CFBG or the fiber-optic dichroic mirror is given by

$$R = R_p \exp\left[-\frac{(\omega-\omega_0)^2}{2\Delta\omega}\right]\exp\left(\frac{iD_2}{2}\omega^2\right) \tag{3}$$

where, R_p is the peak reflectivity of the CFBG or the dielectric thin film output coupler, ω is the optical frequency of the laser, ω_0 and $\Delta\omega$ are the center frequency and the 3-dB bandwidth of the CFBG or the dielectric thin film output coupler respectively, D_2 is the second-order dispersion of the CFBG and is zero for the dielectric thin film output coupler.

The nonlinear absorption dynamics of the SA can be described as [62],

$$\frac{dq(t)}{dt} = -\frac{q(t)-q_0}{\tau_A} - q(t)\frac{|A(t)|^2}{E_A} \tag{4}$$

where, E_A and τ_A are the saturation energy and the recovery time of the SA, respectively. It is noted that τ_A of the SA for GHz repetition rate FML-AFLs should be much less than the round-trip of the ultra-short fiber cavity. q_0 is the non-saturable loss of the SA.

In the simulation, the light circulates in the fiber cavity shown in Fig. 1 and stationary output can be obtained until that when the iteration is converged. The criterion for the converge of the iteration is given by

$$\varepsilon = \frac{\sqrt{\sum_{k=1}^{N}\left[A(k)^2 - A'(k)^2\right]^2}}{\sum_{k=1}^{N}A(k)^2} < 10^{-5} \tag{5}$$

where $A(k)$ is the amplitude of a data point describing the pulse shape of the current loop and $A'(k)$ is that of the previous loop, N is the total number of the element of the matrix over entire time window, and k is the element number. N is 2^{18} in our simulation. Therefore, the criterion for a stable output is that the normalized difference between the shapes of two sequent pulses is less than 10^{-5}. It should be noted that Q-switched mode-locking cannot be simulated with this model and is considered as an unstable output in our simulation. Q-switched mode-locking of a fiber laser can be modeled when the Q-switched operation is combined with the

Optics EXPRESS

mode-locking operation, which needs to solve the rate equations for specific gain medium and thus is out of the scope of this paper. However, in addition to continuous-wave (CW) mode-locking, pulsation mode-locking, multi-pulse mode-locking, and harmonic mode-locking can be simulated with this model. Here, we define a parameter d to evaluate the instability of a mode-locked laser, which can be described as

$$d = \frac{A_{\max} - A_{\min}}{A_{\max}}$$

$$\mathrm{A_{max}} = \max\{\text{pulse peak 1, pulse peak 2, pulse peak 3, …, pulse peak n}\},\ \mathrm{n} = 1000, \quad (6)$$

$$\mathrm{A_{min}} = \min\{\text{pulse peak 1, pulse peak 2, pulse peak 3, …, pulse peak n}\},\ \mathrm{n} = 1000.$$

Therefore, d is the variation of the peak powers of a pulse train. Here, we define the fundamentally mode-locked operation of the all-fiber laser as CW mode-locking or highly stable mode-locking when d is smaller than 10^{-3} (the deep blue regions in following color maps) and as pulsation mode-locking for $d > 10^{-3}$.

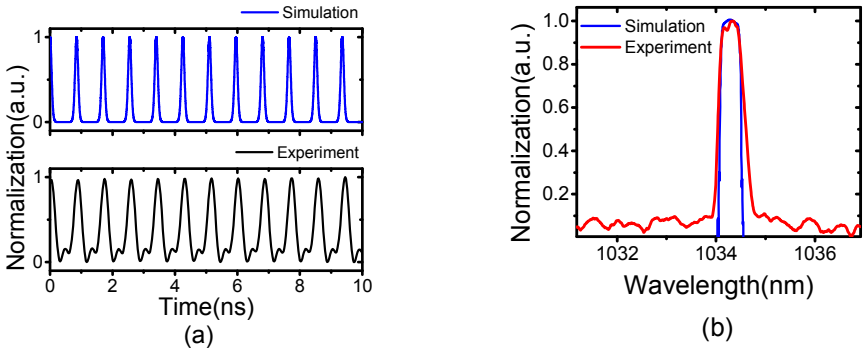

Fig. 2. (a) Pulse trains and (b) Optical spectra of the simulation and experiment of a 1-GHz repetition rate fundamentally mode-locked all-fiber laser.

To verify the reliability and applicability of the modeling, we simulated a 1 GHz repetition rate FML-AFL at 1034 nm that was developed in our lab. The AFL was developed by splicing a 5-cm 6 wt% Yb^{3+}-doped phosphate fiber to a CFBG with a reflectivity of 61% and a 3-dB bandwidth of 5 nm. The dispersion of the CFBG is about 0.37 ps^2. The other end of the Yb^{3+}-doped phosphate fiber was butt-coupled to a SESAM with a saturation fluence of 70 μJ/cm^2, a modulation depth of 3%, and a linear absorption of 5%. The measured and simulated pulse trains and optical spectra of the laser are shown in Figs. 2(a) and 2(b), respectively. The time window for the simulation was set to be 1 ns and the pulse train was obtained by recording the output of the FML-AFL for many loops when stable mode-locking was formed. Clearly, the simulation results are in a great agreement with the experimental results, verifying the correctness and reliability of the modeling.

3. Simulation results and discussion

In this section, the simulation results of GHz repetition rate mode-locked AFLs are presented and discussed. The performance of an AFL with a total cavity length of 10 cm, consisting of a 5-cm gain fiber, a 1-cm CFBG, and a 4-cm passive SMF, was first simulated. The gain fiber has a dispersion parameter of −36 ps/nm/km and a nonlinear coefficient of 4 $W^{-1}km^{-1}$. Its gain saturation energy and bandwidth were assumed to be 100 pJ and 20 nm, respectively. The SMF length has a dispersion parameter of −38 ps/nm/km and a nonlinear coefficient of 6 $W^{-1}km^{-1}$. The SA has a saturation energy of 100 pJ, a recovery time of 2 ps, and a non-

Optics EXPRESS

saturable loss of 5%. The dispersion of the SA is −5000 fs^2. The total net cavity dispersion (D_{total}) is determined by $D_{total} = D_{CFBG} + D_{2,SMF} \cdot L_{SMF} + D_{2,gain} \cdot L_{gain} + D_{SA}$. Because the dispersion of a CFBG can be tailored with various designs, D_{total} can be varied in a large range from negative dispersion (anomalous dispersion) to positive dispersion (normal dispersion) by just using a proper CFBG. In our modeling, we assume that D_{total} can be in a range of −0.1 to −1 ps^2 for the anomalous dispersion (AD) regime and in a range of 0.1 to 1 ps^2 for the normal dispersion (ND) regime.

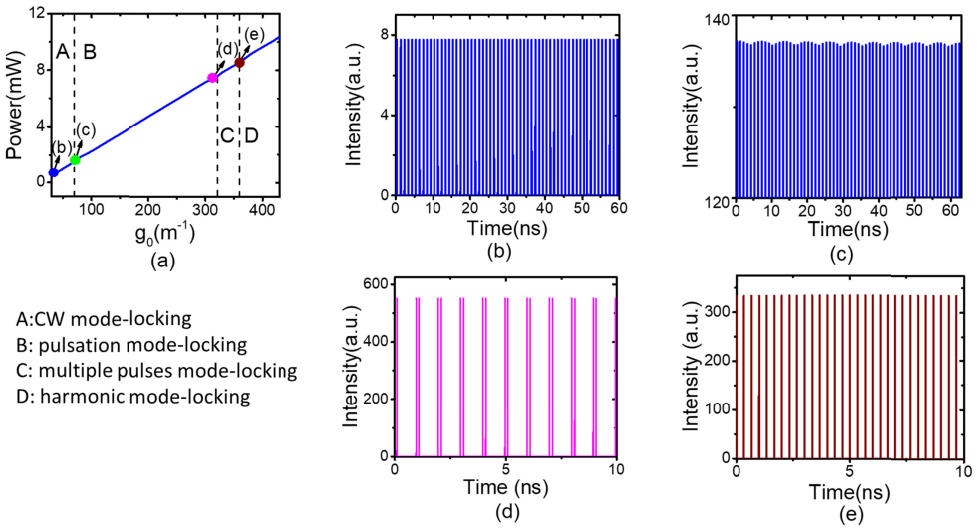

Fig. 3. Simulation results of a 10-cm-long all-fiber laser incorporated with an SESAM operating with different small signal gains (different power powers), (a) Output power of the all-fiber laser as a function of small signal gain; (b) Pulse train of CW mode-locking when g_0 is 30 m^{-1}, (c) Pulse train of pulsation mode-locking when g_0 is 70 m^{-1}, (d) Pulse train of two-pulse mode-locking when g_0 is 320 m^{-1}, (e) Pulse train of 3rd order harmonic mode-locking when g_0 is 360 m^{-1}.

Generally, a fiber laser incorporated with a SA can operate at different pulse states, such as random pulsed oscillation, Q-switched operation, Q-switched mode-locking, CW mode-locking, pulsation mode-locking, multi-pulse mode-locking and harmonic mode-locking, depending on the cavity parameters and pump power. These operation states can be modeled by solving the nonlinear Schrödinger equation and nonlinear absorption dynamics of the SA in section 2 with the existing computing technique. The laser performance of a 10-cm long all-fiber Yb^{3+} laser incorporated with an SESAM with a modulation depth of 5% and a saturation fluence of 70 μJ/cm^2 was simulated for a small signal gain g_0 range of 10 m^{-1} to 500 m^{-1} and is shown in Fig. 3. In the simulation, D_{total} and R were set to be −1 ps^2 and 70%, respectively. The output power as a function of the small signal gain g_0 is shown in Fig. 3(a). The threshold of g_0 for this laser is 10 m^{-1}. Fundamental mode-locking (FML) starts at a g_0 of 30 m^{-1} and maintain till g_0 exceeds 320 m^{-1}. Clearly, the pump power range for fundamental mode-locking is much larger than what we observed in a regular MHz repetition rate mode-locked fiber because the accumulated nonlinearity B∝P_p*L of a GHz repetition rate mode-locked fiber laser is at least 4 orders of magnitude smaller than that of a MHz repetition rate mode-locked fiber laser. A typical pulse train of CW mode-locking is shown in Fig. 3(b). However, the instability of FML increases with the increase of g_0 and the operation becomes pulsation mode-locking. As shown in Fig. 3 (c), the instability of the FML is 0.72% when g_0 is 70 m^{-1}. The FML stability degrades with the increased g_0 and multi-pulse mode-locking

starts as g_0 is greater than 320 m^{-1}. The pulse train of two-pulse mode-locking at a g_0 of 320 m^{-1} is shown in Fig. 3(d). Harmonic mode-locking is obtained when g_0 is between 360 m^{-1} and 430 m^{-1} and the pulse train of 3rd-order harmonic mode-locking is shown in Fig. 3(e). As g_0 exceeds 430 m^{-1}, a stable mode-locking state can't be achieved any more. Because FML of an AFL is more interesting than multi-pulse mode-locking for most of practical applications, we will only present the simulation and analysis of CW mode-locking and pulsation mode-locking of short-length AFLs in the following sections.

3.1 1-GHz repetition rate FML-AFLs operating at AD-regime

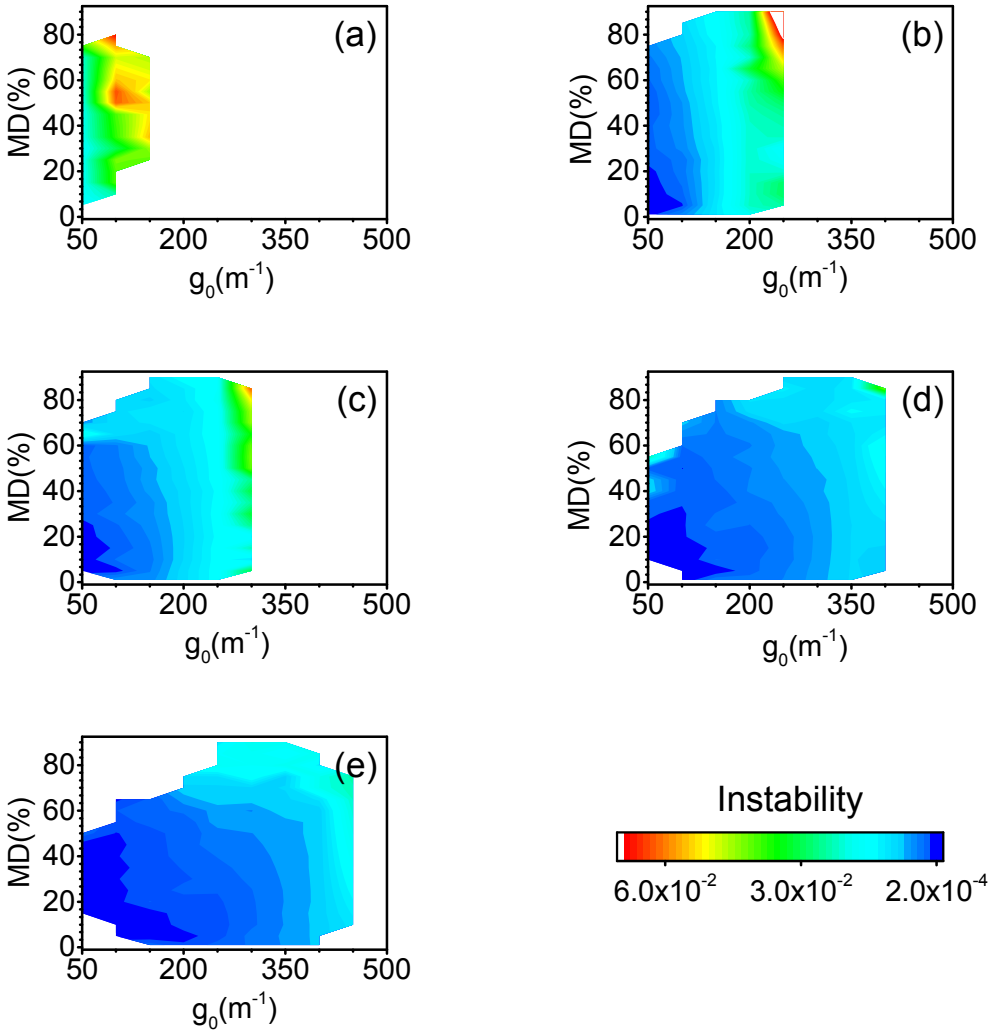

Fig. 4. The calculated instability as a function of g_0 and MD for 1-GHz repetition rate FML-AFLs with the total net cavity dispersion of (a) D_{total} = –0.1 ps^2, (b) D_{total} = –0.3 ps^2, (c) D_{total} = –0.5 ps^2, (d) D_{total} = –0.8 ps^2 and (e) D_{total} = –1 ps^2.

In this subsection, the performance of 1-GHz repetition rate FML-AFLs operated at AD-regime is numerically studied. The instability of the FML-AFLs as a function of g_0 and MD for different D_{total} was calculated and is presented in Fig. 4. The reflectivity of the CFBG was set as 70%. The g_0 and MD are set in ranges of 50 m^{-1} to 500 m^{-1} and 1% to 90%, respectively. The contour plots of the FML instabilities for D_{total} of –0.1 ps^2, –0.3 ps^2, –0.5 ps^2, –0.8 ps^2, and –1 ps^2, are shown in Figs. 4(a)-4(e), respectively. In agreement with the

Optics EXPRESS

experimental observation [57], highly stable mode-locking can be only obtained at a small range of pump power (g_0) and the stability of an FML-AFL degrades with the increased pump power (g_0).

It can be seen from Figs. 4(a)-4(e) that the ranges of g_0 and MD for stable FML increase with the increased anomalous dispersion of the fiber cavity. In other words, the conditions for stable 1-GHz repetition rate FML-AFLs is more flexible when the net cavity dispersion is anomalous and has a large value such that the interaction of dispersion and nonlinear effect can result in stable soliton pulses. The deep blue regions shown in Figs. 4(b)-4(e) indicate that highly stable fundamental mode-locked pulses at a repetition rate of 1 GHz can be achieved by choosing a proper MD less than 50% and managing the cavity dispersion properly. When the D_{total} is small and close to zero, the ranges of g_0 and MD for stable mode-locking are very small and the instabilities of the mode-locking are large as shown in Fig. 4(a), which is similar to the observation of MHz repetition rate FML. Therefore, deliberate design of an AFL with a small net anomalous cavity dispersion is very critical to achieve stable FML operation.

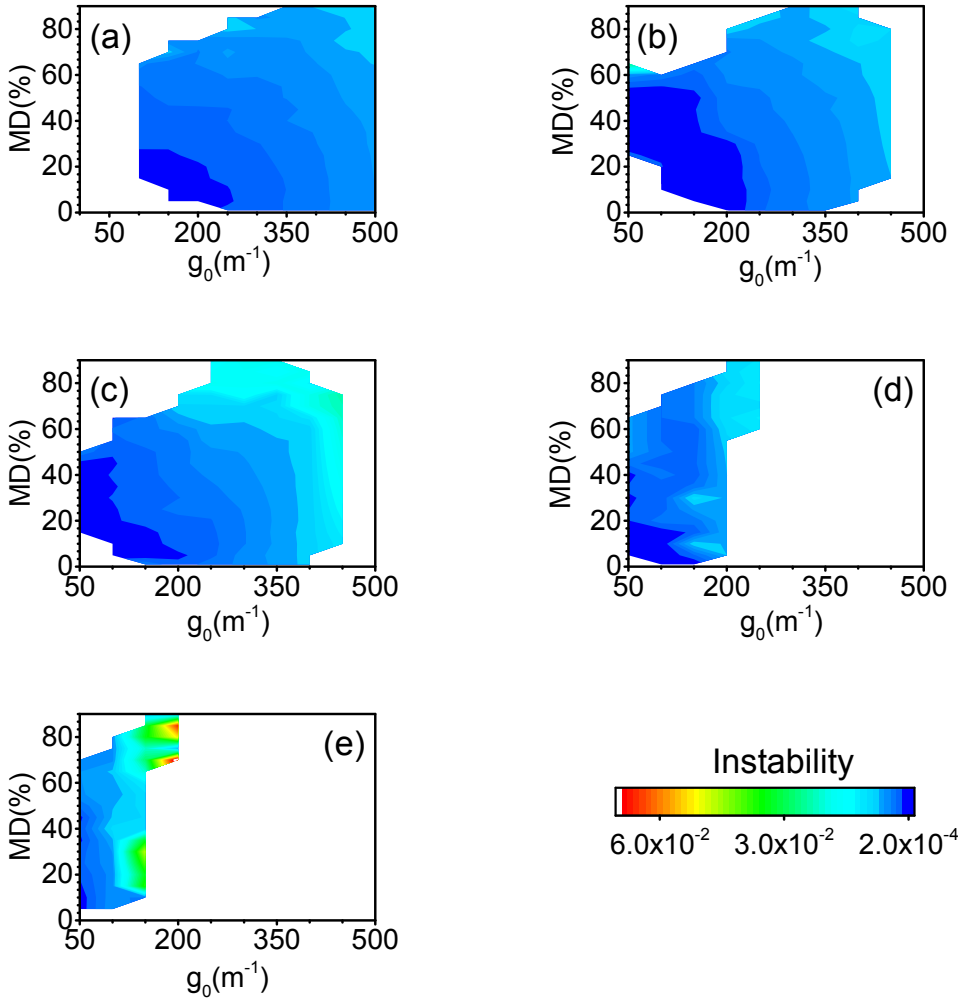

Fig. 5. The calculated instability as a function of g_0 and MD for 1-GHz repetition rate FML-AFLs with a net cavity dispersion of −1 ps^2 and with the output coupler reflectivity of (a) R = 30%, (b) R = 50%, (c) R = 70%, (d) R = 80%, and (e) R = 90%.

Optics EXPRESS

Another key parameter determining the stability of an FML-AFL is the R of the output coupler of the cavity. Figure 5 shows the calculated instabilities of 1-GHz repetition rate FML-AFLs with varied R. The net cavity dispersion for this calculation was set as -1 ps^2. The contour plots of the instabilities of the FML for R of 30%, 50%, 70%, 80%, and 90%, are shown in Figs. 5(a)-5(e), respectively. It is clear that the ranges of MD and g_0 for stable mode-locking reduce with the increased R. When the R is 90%, the ranges of MD and g_0 for stable mode-locking is very small and the instability of the mode-locking is large. This is because the power intensity of the laser inside the cavity increases with the increased reflectivity of the output coupler and the interaction of the dispersion and nonlinear effects is hard to arrive in a stable soliton operation. The deep blue regions shown in Figs. 5(a)-5(d) tell us that highly stable fundamental mode-locked pulses at a repetition rate of 1 GHz can be achieved by choosing a proper SA with a MD < 55% and the ranges of MD and g_0 for stable mode-locking are large when the R of the CFBG or fiber-optic dichroic mirror is 50%.

The pulse width, spectral bandwidth, and time-bandwidth product (TBP) of the stable mode-locked pulses generated by the 1-GHz repetition rate FML-AFLs operating at the AD-regime as a function of the g_0, R, D_{total}, and MD were calculated and are plotted in Fig. 6. Figure 6(a) shows the three parameters of the pulses as a function of the g_0 when the R = 70%, MD = 20%, D_{total} = –0.5 ps^2. It is clear that the pulse width deceases while the spectral bandwidth increases with the increased g_0. The TBP decreases with the increased g_0 and arrives in a transform-limited value eventually. It should be noted that this conclusion can be applied only for a specific range of g_0 in which stable fundamental mode-locking can be achieved. Further increase of g_0 will arrive in unstable or multi-pulse mode-locking. Figure 6(b) shows the three parameters of the pulses as a function of the R when g_0 = 100 m^{-1}, MD = 20%, D_{total} = –0.5 ps^2. Similar to the case of increasing g_0, both the pulse width and TBP decrease while the spectral width increases with the increased R. Figure 6(c) shows the three parameters of the pulses as a function of D_{total} when R = 70%, MD = 20%, g_0 = 100 m^{-1}. The calculation results agree well with the general observation and understanding of mode-locked fiber lasers, i.e., the pulse width decreases while the spectral bandwidth increases as the net cavity dispersion reduces. Sub-ps pulses can be achieved when the cavity dispersion approaches zero by careful dispersion management. The TBP is nearly independent of the net cavity dispersion and has the value close to that of transform-limited. Figure 6(d) shows the three parameters of the pulses as a function of the MD when g_0 = 100 m^{-1}, R = 70%, D_{total} = –0.5 ps^2. The pulse width decreases and the spectral bandwidth increases with the increased MD. The TBP of the output pulses increases from the value of transform-limited soliton pulses to more than 0.6, indicating that the pulses are chirped as the MD increases.

Optics EXPRESS

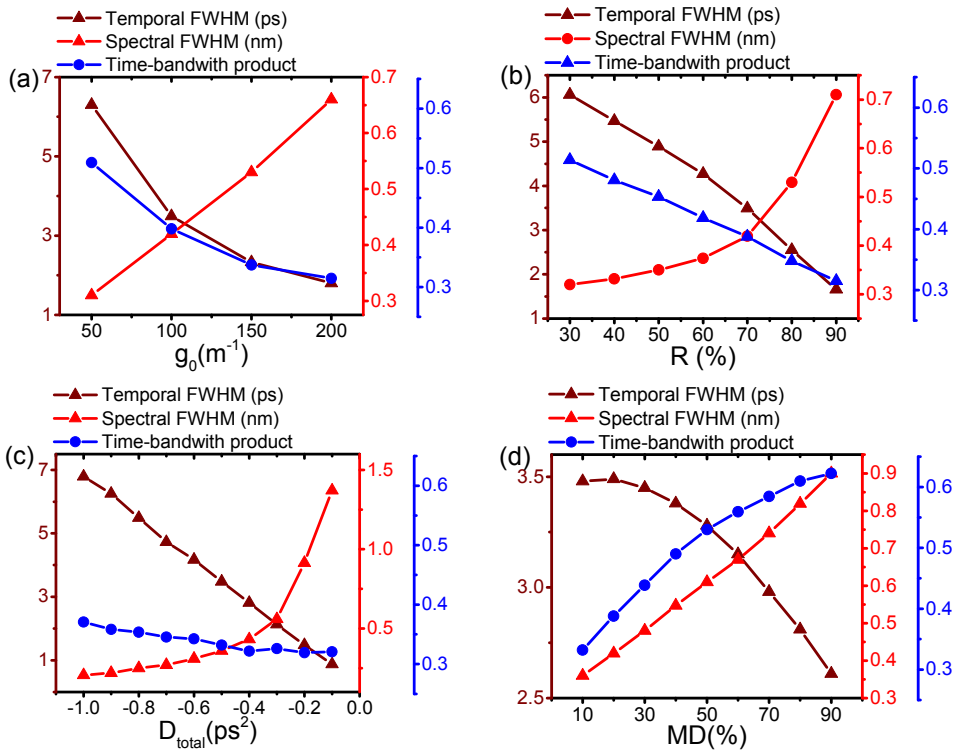

Fig. 6. Calculated pulse width, spectral bandwidth, and TBP of the 1-GHz repetition rate FML-AFLs operating in the AD-regime with (a) g_0 = 50~200 m^{-1}, R = 70%, MD = 20%, D_{total} = –0.5 ps^2, (b) R = 30% ~90%, g_0 = 100 m^{-1}, MD = 20%, D_{total} = –0.5 ps^2, (c) D_{total} = –0.1~-1 ps^2, R = 70%, MD = 20%, g_0 = 100 m^{-1}, (d) MD = 10% to 90%, g_0 = 100 m^{-1}, R = 70%, D_{total} = –0.5 ps^2.

3.2 1-GHz repetition rate FML-AFLs operating at ND-regime

In this subsection, the performance of 1-GHz repetition rate FML-AFLs operating in the ND-regime are numerically studied. The mode-locking instability of the laser as a function of g_0 and MD for different D_{total} was calculated and is presented in Fig. 7. The R and spectral bandwidth of the CFBG are set to be 70% and 5 nm, respectively. The varying ranges of g_0 and MD are 50 m^{-1} ~500 m^{-1} and 1% ~90%, respectively. The contour plots of the instabilities of the FML as a function of g_0 and MD for D_{total} of 0.1 ps^2, 0.3ps^2, 0.5ps^2, 0.8ps^2, and 1ps^2, are shown in Figs. 7(a)-7(e), respectively. In agreement with the experimental observation [46], stable mode-locking of the AFLs can usually be achieved in large ranges of g_0 and MD.

The ranges of g_0 and MD for stable FML decrease a bit with the increased D_{total}. The deep blue regions shown in Figs. 7(a)-7(e) indicate that highly stable fundamental mode-locked pulses at a repetition rate of 1 GHz can be achieved at large pump powers (large g_0) as the MD is large. When the total net cavity dispersion is 1 ps^2, the ranges of g_0 and MD for highly stable mode-locking are much smaller than those of the other cases and the instability of the FML is due to the large chirp [54].

Optics EXPRESS

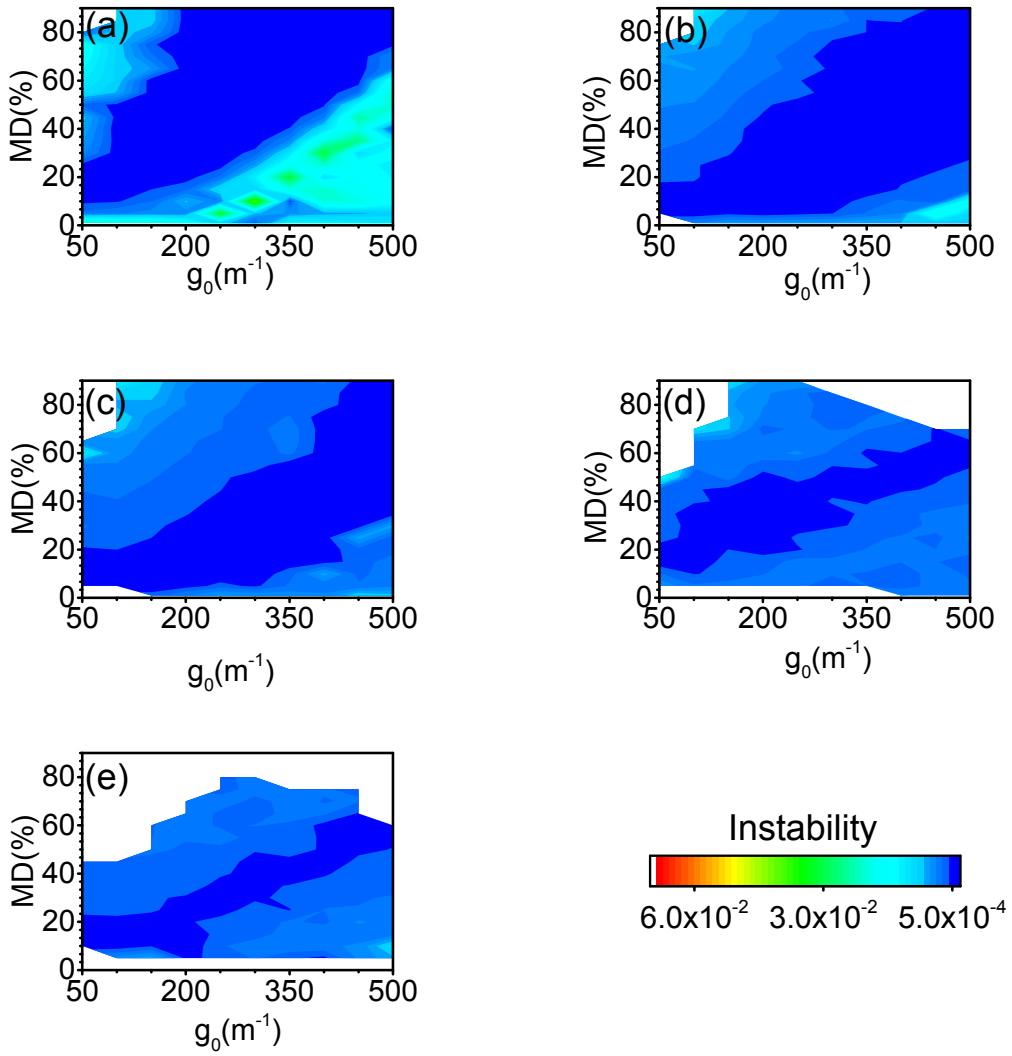

Fig. 7. The calculated instability as a function of g_0 and MD for 1-GHz repetition rate FML-AFLs with a total net cavity dispersion of (a) D_{total} = 0.1 ps^2, (b) D_{total} = 0.3 ps^2, (c) D_{total} = 0.5 ps^2, (d) D_{total} = 0.8 ps^2, (e) D_{total} = 1 ps^2.

Compared to the FMLs at the AD-regime shown in Fig. 4, FMLs operating at the ND-regime can be achieved in much larger ranges of g_0 and MD as shown in Fig. 7. This is consistent with the experimental observations [46] that stable fundamental normal dispersion mode-locking can be obtained at a very large range of pump power while anomalous dispersion mode-locking can be achieved only at a small range of pump power.

Optics EXPRESS

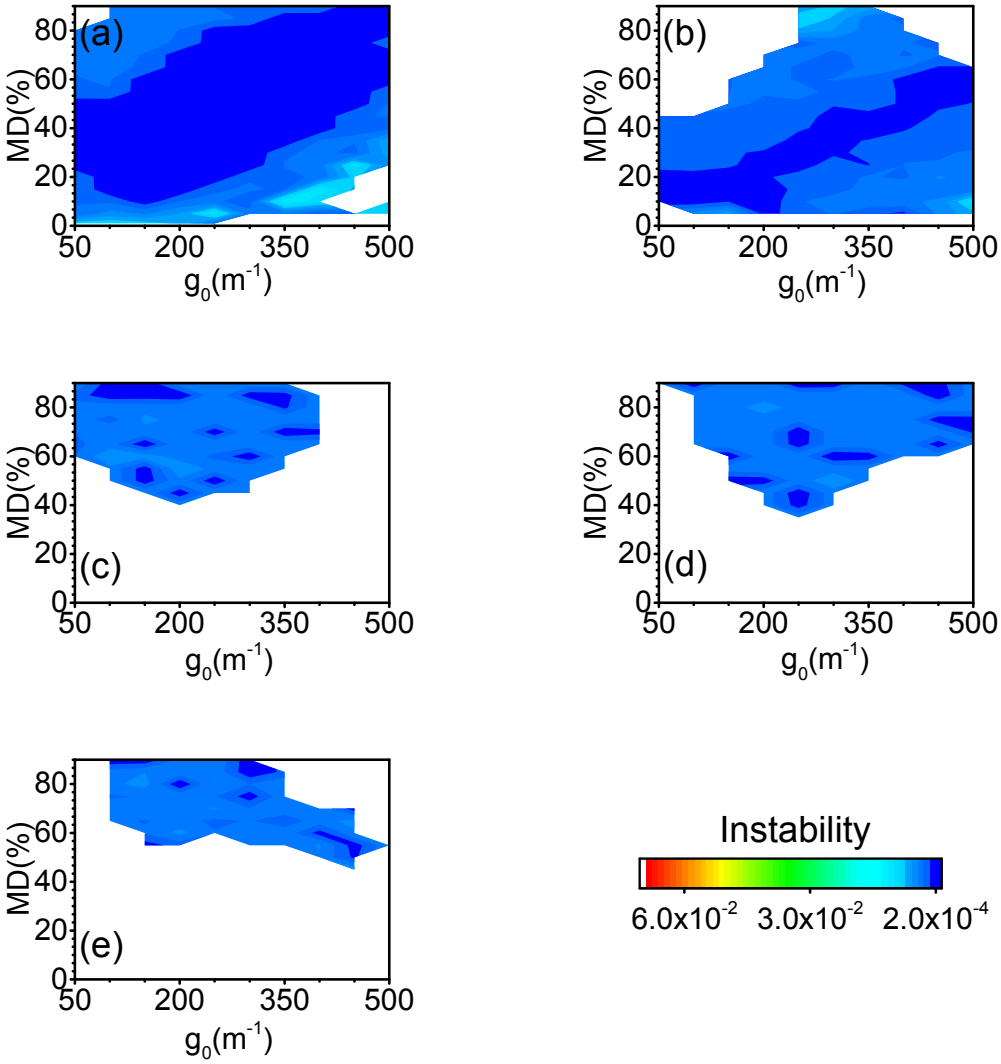

Fig. 8. The calculated instability as a function of g_0 and MD for 1-GHz repetition rate FML-AFLs with a D_{total} of 1 ps^2 when the spectral bandwidth of the CFBG is (a) BW = 1 nm, (b) BW = 5 nm, (c) BW = 10 nm, (d) BW = 20 nm and (e) BW = 30 nm.

Spectral filtering effect is a key requirement for self-started mode-locking in the ND-regime [41]. The mode-locking instability of the AFLs as a function of g_0 and MD was calculated for different spectral bandwidths (BWs) of the CFBG and is presented in Fig. 8. The total net cavity dispersion is set as 1 ps^2. The contour plots of the instabilities of the FMLs as a function of g_0 and MD for BW of 1 nm, 5 nm, 10 nm, 20 nm, and 30 nm, are calculated and shown in Figs. 8(a)-8(e), respectively. Clearly, stability of the mode-locking decreases with the increased BW. When the BW is small, highly stable mode-locking can be achieved in a large range of g_0 and MD. As the BW exceeds 10 nm, highly stable fundamental mode-locked pulses are available only at some specific cases and the MD of a SA for stable mode-locking needs to be > 35%, as shown in Figs. 8(c)-(e).

Optics EXPRESS

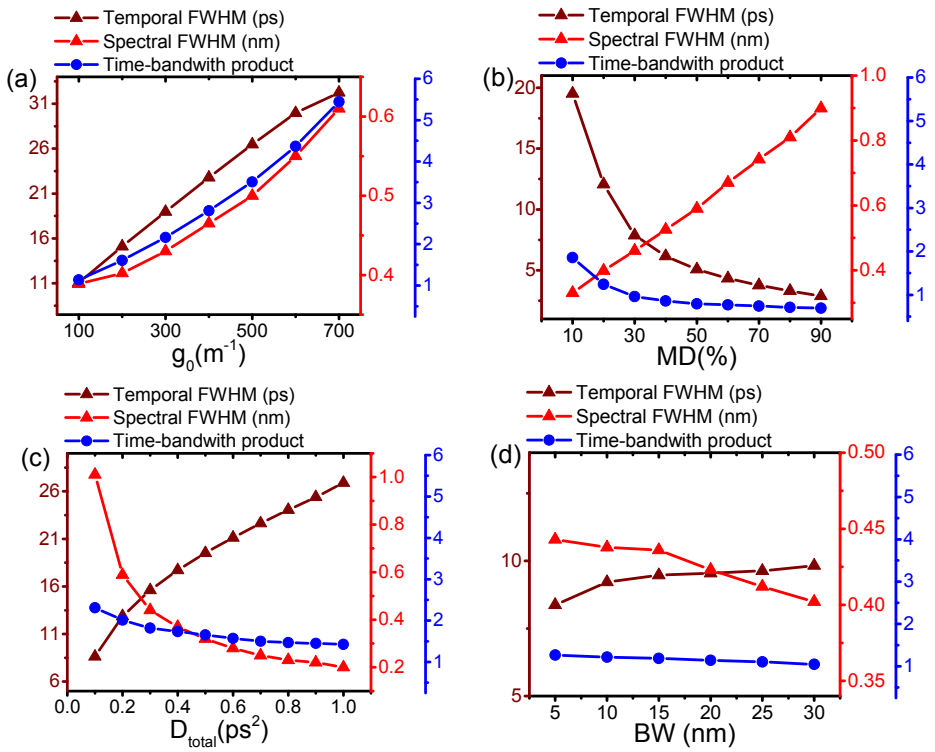

Fig. 9. Calculated pulse width, spectral bandwidth, and TBP of the 1- GHz repetition rate FML-AFLs operating in the ND-regime with (a) g_0 = 100~700 m^{-1}, R = 70%, MD = 20%, D_{total} = 0.5 ps^2, (b) MD = 10% ~90%, g_0 = 100 m^{-1}, R = 70%, D_{total} = 0.5 ps^2, (c) D_{total} = 0.1~1 ps^2, R = 70%, MD = 20%, g_0 = 100 m^{-1} and (d) BW = 5 to 30 nm, g_0 = 300 m^{-1}, MD = 60%, R = 70%, D_{total} = 0.5 ps^2.

The pulse width, spectral bandwidth, and TBP of the pulses generated by the 1-GHz repetition rate FML-AFLs operated in the ND regime as a function of g_0, MD, D_{total}, and BW were calculated and are plotted in Fig. 9. Figure 9(a) shows the three parameters of the mode-locked pulses as a function of the g_0, when the R = 70%, MD = 20%, D_{total} = 0.5 ps^2, BW = 5 nm. It is consistent with the experimental observations [41] that all the three parameters increase with the increased g_0 and the pulses are highly chirped at high pump power levels. Figure 9(b) shows the three parameters of the mode-locked pulses as a function of the MD when g_0 = 100 m^{-1}, R = 70%, and D_{total} = 0.5 ps^2, BW = 5 nm. Both the pulse width and TBP decrease while the spectral width increases with the increased MD. Figure 9(c) shows the three parameters of the mode-locked pulses as a function of the D_{total} when R = 70%, MD = 20%, g_0 = 100 m^{-1}, BW = 5 nm. The pulse width increases while both the spectral bandwidth and TBP decreases with the decreased D_{total}. Figure 9(d) shows the three parameters as a function of the BW when g_0 = 300 m^{-1}, MD = 60%, R = 70%, D_{total} = 0.5 ps^2. Pulse width increases while spectral width decreases with the increased BW of the CFBG. TBP of the pulses, however, doesn't changes much, which is consistent with the results presented in [30], indicating the filtering effect of the CFBG do help for avoiding the break-up of the pulses mode-locked in the ND regime.

3.3 Instability of fundamental mode-locking at higher GHz repetition rates

In this subsection, FML-AFLs operating at higher GHz repetition rates are numerically investigated and studied. Since the cavity length needs to be several centimeters or sub-cm,

the all-fiber cavity consists of only a short gain fiber, a DC and a SA, as shown in Fig. 1(b). The parameters of the gain fiber and SA are set the same values as above. The total dispersion of the cavity is calculated by $D_{total} = D_{DC} + D_{gain} + D_{SA}$. Because the dispersion of the DC is negligible, that of the gain fiber dispersion is generally hundreds of fs^2, and that of the SA dispersion is around a few thousands of fs^2, the D_{total} is set as −5000 fs^2 and + 5000 fs^2 for the ND and AD mode-locking regimes, respectively. The varying ranges of g_0 and MD are 50 ~1000 m^{-1} and 1% ~90%, respectively.

Firstly, the instabilities of FML-AFLs operating in the AD-regime with repetition rates of 5 GHz, 10 GHz, and 20 GHz are calculated and plotted as a function of g_0 and MD by the contour figures shown in Fig. 10. It can be seen from Figs. 10(a)-10(c) that the instability of the FML-AFLs decreases while the ranges of g_0 and MD for the stable FML increase with the increased repetition rate. This is because the peak intensity of the mode-locked pulses becomes smaller as the repetition rate increases. It tells us that stable mode-locking can be obtained at larger ranges of g_0 and MD of the SA when the repetition rate is higher. It is also consistent with the experimental observation [26] that CW fundamental mode-locking can be only achieved with SAs with very small MD.

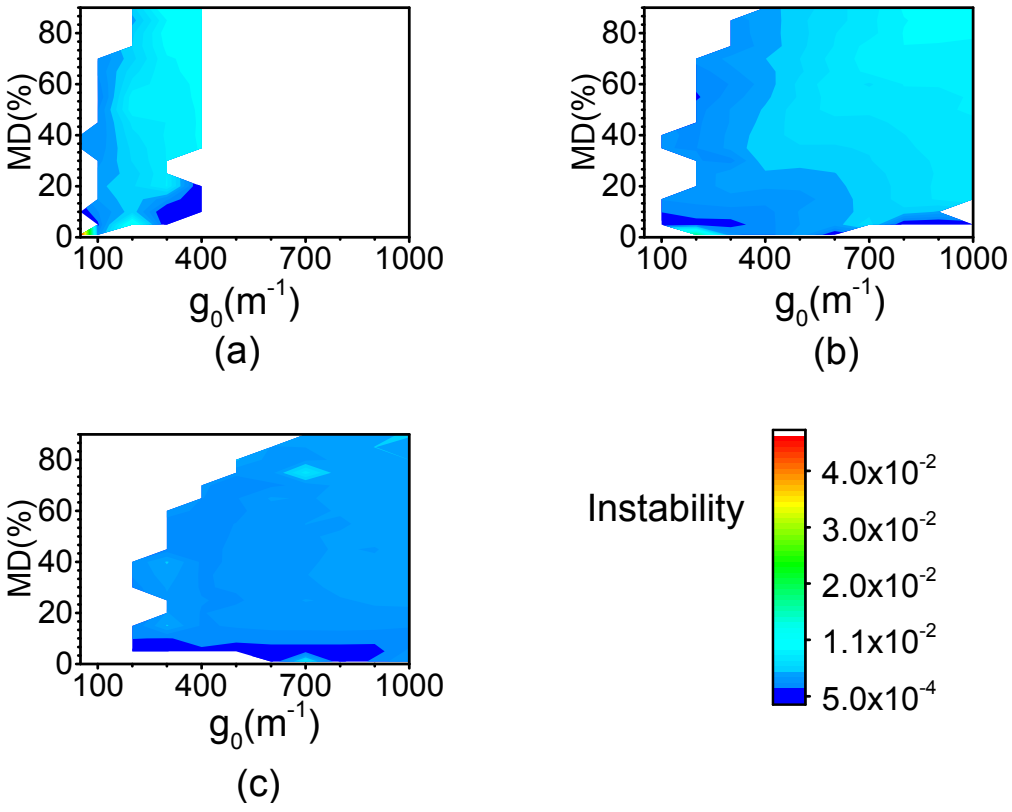

Fig. 10. The calculated instability as a function of g_0 and MD for the FML-AFLs operating in the AD-regime with a repetition rate of (a) 5 GHz, (b) 10 GHz and (c) 20 GHz, D_{total} of −5000 fs^2, and R of 70%.

Then the instabilities of FML-AFLs operating in the ND-regime with repetition rates of 5 GHz, 10 GHz, and 20 GHz were calculated and are shown by the contour plots in Fig. 11. It is clearly that the ranges of the g_0 and MD for stable mode-locking decrease with the increased repetition rate. The MD of the SA required for highly stable mode-locking also decreases with the increased repetition rate. Therefore, proper selection of a SA is very

Optics EXPRESS

critical for developing a highly stable mode-locked AFL operating at 10-20 GHz repetition rate.

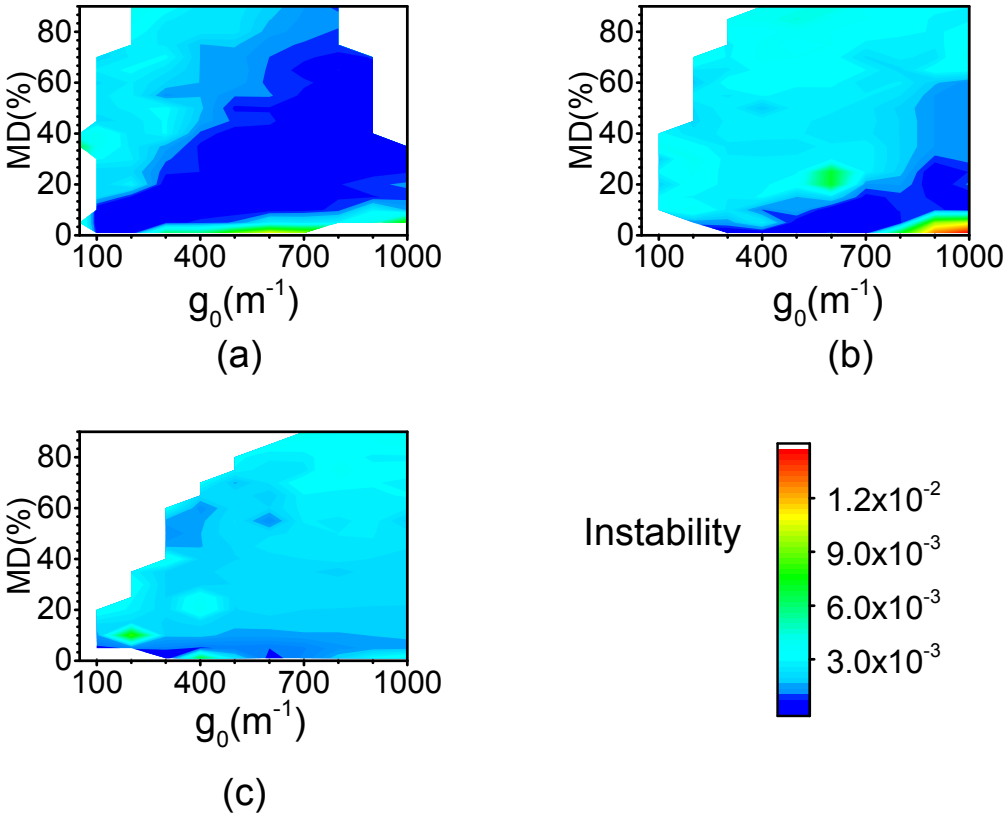

Fig. 11. The calculated instability as a function g_0 and MD for the FML-AFLs operating in the ND-regime with a repetition rate of (a) 5 GHz, (b) 10 GHz and (c) 20 GHz, D_{total} of 5000 fs^2, and R of 70%.

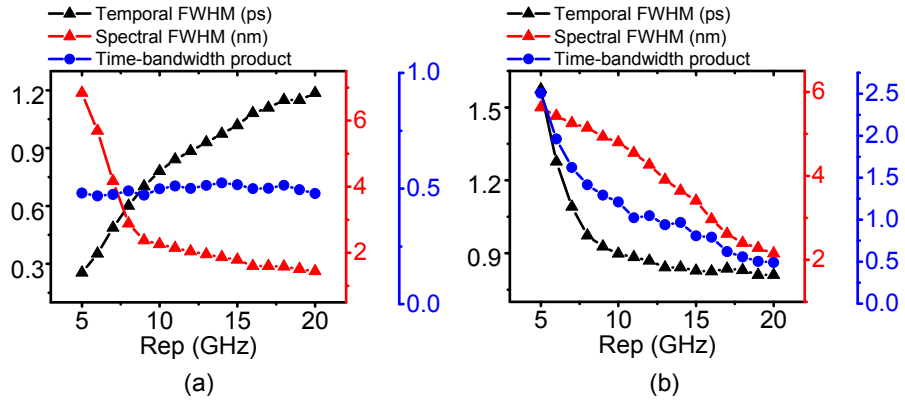

Fig. 12. Calculated pulse width, spectral bandwidth, and TBP of the FML-AFLs operating at different repetition rates for (a) g_0 = 200 m^{-1}, R = 70%, MD = 15%, D_{total} = –5000 fs^2 and (b) g_0 = 200 m^{-1}, R = 70%, MD = 15%, D_{total} = 5000 fs^2.

The pulse width, spectral bandwidth, and TBP of the FML-AFLs operating in the AD and ND regimes at repetition rates varying from 5 GHz to 20 GHz are calculated and are shown in

Optics EXPRESS

Figs. 12(a) and 12(b), respectively. It can be seen from Fig. 12(a) that the pulse width increases while the spectral bandwidth decreases with the increased repetition rate, and the TBPs of the FML-AFLs don't change much as the repetition rate increases because they operate in soliton mode-locking. As shown in Fig. 12(b), when the FML-AFLs operate in the ND-regime, the TBP, pulse width, and spectral bandwidth, however, decrease with the increase of the repetition rate.

4. Conclusion

Performance of GHz repetition rate mode-locked AFLs was numerically investigated and the instability of FMLs in terms of total net cavity dispersion, small-signal gain, spectral bandwidth, and MD of the SA were studied. The simulation results show that, when the net cavity dispersion is negative (anomalous dispersion), highly stable FML can be achieved in small specific ranges of MD of the saturable absorber and the small signal gain of the active fiber and the ranges becomes large as the net cavity dispersion becomes large or the reflectivity of the output coupler becomes small. As the net cavity dispersion is positive (normal-dispersion), highly stable FML can be obtained in large ranges of MD of the saturable absorber and the small signal gain of the active fiber and the stability of the mode-locking doesn't change much with the net cavity dispersion. A narrow bandwidth of the CFBG or fiber-optic dichroic mirror is helpful for achieving highly stable mode-locking in the ND regimes. The ranges of modulation depth and small signal gain for stable FML decrease with the increased repetition rate of the FML. The highly stable FML at high GHz repetition rate can be obtained only with small MD of the SA for the mode-locking at both AD and ND regimes. The simulation results are consistent with the reported experimental observations that the MD of the SA and small signal gain ranges of stable mode-locking at normal dispersion are much larger than those at anomalous dispersion. The small signal gain range for a GHz repetition rate FML is much larger than what we usually observed with a MHz repetition rate FML [51] because the accumulated nonlinearity of a GHz repetition rate FML is at least 4 orders of magnitude smaller.

The simulation results are very helpful for the design and development of GHz repetition rate FML-AFLs that can be used for a variety of applications. The numerical investigation can also help us to understand the pulsed laser performance in short-cavity all-fiber lasers.

Funding

National Science Foundation Engineering Research Center for Integrated Access Networks (#EEC-0812072); Technology Research Initiative Fund (TRIF) Photonics Initiative of the University of Arizona.; National Natural Science Foundation of China (NSFC) (61575075).

Acknowledgments

We would like to thank Chinese Scholarship Council for financial support.

References

1. U. Keller, "Recent developments in compact ultrafast lasers," Nature **424**(6950), 831–838 (2003).
2. N. Ji, J. C. Magee, and E. Betzig, "High-speed, low-photodamage nonlinear imaging using passive pulse splitters," Nat. Methods **5**(2), 197–202 (2008).
3. S. W. Chu, T. M. Liu, C. K. Sun, C. Y. Lin, and H. J. Tsai, "Real-time second-harmonic-generation microscopy based on a 2-GHz repetition rate Ti:sapphire laser," Opt. Express **11**(8), 933–938 (2003).
4. C.-H. Li, A. J. Benedick, P. Fendel, A. G. Glenday, F. X. Kärtner, D. F. Phillips, D. Sasselov, A. Szentgyorgyi, and R. L. Walsworth, "A laser frequency comb that enables radial velocity measurements with a precision of 1 cm s^{-1}," Nature **452**(7187), 610–612 (2008).
5. S. A. Diddams, L. Hollberg, and V. Mbele, "Molecular fingerprinting with the resolved modes of a femtosecond laser frequency comb," Nature **445**(7128), 627–630 (2007).
6. M. Babaeian, P.-A. Blanche, R. A. Norwood, T. Kaplas, P. Keiffer, Y. Svirko, T. G. Allen, V. W. Chen, S.-H. Chi, J. W. Perry, S. R. Marder, M. A. Neifeld, and N. Peyghambarian, "Nonlinear optical components for all-optical probabilistic graphical model," Nat. Commun. **9**(1), 2128 (2018).

Optics EXPRESS

7. M. Babaeian, P. Keiffer, M. A. Neifeld, R. Thamvichai, R. A. Norwood, P.-A. Blanche, J. Wissinger, and N. Peyghambarian, "Optical Versus Electronic Implementation of Probabilistic Graphical Inference and Experimental Device Demonstration Using Nonlinear Photonics," IEEE Photonics J. **10**(5), 7801412 (2018).
8. S. A. Diddams, "The evolving optical frequency comb," J. Opt. Soc. Am. B **27**(11), B51–B62 (2010).
9. D. A. Braje, M. S. Kirchner, S. Osterman, T. Fortier, and S. A. Diddams, "Astronomical spectrograph calibration with broad-spectrum frequency combs," ," Eur. Phys. J. D **48**(1), 57–66 (2008).
10. G. Chang, C. H. Li, D. F. Phillips, R. L. Walsworth, and F. X. Kärtner, "Toward a broadband astro-comb: effects of nonlinear spectral broadening in optical fibers," Opt. Express **18**(12), 12736–12747 (2010).
11. T. Wilken, G. L. Curto, R. A. Probst, T. Steinmetz, A. Manescau, L. Pasquini, J. I. González Hernández, R. Rebolo, T. W. Hänsch, T. Udem, and R. Holzwarth, "A spectrograph for exoplanet observations calibrated at the centimetre-per-second level," Nature **485**(7400), 611–614 (2012).
12. G. G. Ycas, F. Quinlan, S. A. Diddams, S. Osterman, S. Mahadevan, S. Redman, R. Terrien, L. Ramsey, C. F. Bender, B. Botzer, and S. Sigurdsson, "Demonstration of on-sky calibration of astronomical spectra using a 25 GHz near-IR laser frequency comb," Opt. Express **20**(6), 6631–6643 (2012).
13. T. Steinmetz, T. Wilken, C. Araujo-Hauck, R. Holzwarth, T. W. Hänsch, L. Pasquini, A. Manescau, S. D'Odorico, M. T. Murphy, T. Kentischer, W. Schmidt, and T. Udem, "Laser Frequency Combs for Astronomical Observations," Science **321**(5894), 1335–1337 (2008).
14. L. Krainer, R. Paschotta, S. Lecomte, M. Moser, K. J. Weingarten, and U. Keller, "Compact Nd: YVO4 lasers with pulse repetition rates up to 160 GHz," ," IEEE J. Quantum Electron. **38**(10), 1331–1338 (2002).
15. S. Pekarek, T. Südmeyer, S. Lecomte, S. Kundermann, J. M. Dudley, and U. Keller, "Self-referenceable frequency comb from a gigahertz diode-pumped solid-state laser," Opt. Express **19**(17), 16491–16497 (2011).
16. E. K. Lau, X. Zhao, H. K. Sung, D. Parekh, C. Chang-Hasnain, and M. C. Wu, "Strong optical injection-locked semiconductor lasers demonstrating > 100-GHz resonance frequencies and 80-GHz intrinsic bandwidths," Opt. Express **16**(9), 6609–6618 (2008).
17. D. Lorenser, D. Maas, H. J. Unold, A. R. Bellancourt, B. Rudin, E. Gini, D. Ebling, and U. Keller, "50-GHz passively mode-locked surface-emitting semiconductor laser with 100-mW average output power," IEEE J. Quantum Electron. **42**(8), 838–847 (2006).
18. K. Yin, B. Zhang, W. Yang, H. Chen, S. Chen, and J. Hou, "Flexible picosecond thulium-doped fiber laser using the active mode-locking technique," Opt. Lett. **39**(14), 4259–4262 (2014).
19. S. S. Jyu, L. G. Yang, C. Y. Wong, C. H. Yeh, C. W. Chow, H. K. Tsang, and Y. Lai, "250-GHz Passive Harmonic Mode-Locked Er-Doped Fiber Laser by Dissipative Four-Wave Mixing With Silicon-Based Micro-Ring," IEEE Photonics J. **5**(5), 7 (2013).
20. T. Sylvestre, S. Coen, P. Emplit, and M. Haelterman, "Self-induced modulational instability laser revisited: normal dispersion and dark-pulse train generation," Opt. Lett. **27**(7), 482–484 (2002).
21. D. Mao, X. Liu, Z. Sun, H. Lu, D. Han, G. Wang, and F. Wang, "Flexible high-repetition-rate ultrafast fiber laser," Sci. Rep. **3**(1), 3223 (2013).
22. M. Peccianti, A. Pasquazi, Y. Park, B. E. Little, S. T. Chu, D. J. Moss, and R. Morandotti, "Demonstration of a stable ultrafast laser based on a nonlinear microcavity," Nat. Commun. **3**(1), 765 (2012).
23. J. J. McFerran, L. Nenadovic, W. C. Swann, J. B. Schlager, and N. R. Newbury, "A passively mode-locked fiber laser at 1.54 mum with a fundamental repetition frequency reaching 2 GHz," Opt. Express **15**(20), 13155–13166 (2007).
24. I. Hartl, H. A. McKay, R. Thapa, B. K. Thomas, L. Dong, and M. E. Fermann, "GHz Yb-femtosecond-fiber laser frequency comb," in Conference on Lasers and Electro-Optics/Quantum Electronics and Laser Science Conference (IEEE 2009), pp. 582–583.
25. I. Hartl, A. Romann, and M. E. Fermann, "Passively Mode Locked GHz Femtosecond Yb-Fiber Laser Using an Intra-Cavity Martinez Compressor," in 2011 Conference on Lasers and Electro-Optics, (IEEE 2011).
26. H. W. Chen, G. Chang, S. Xu, Z. Yang, and F. X. Kärtner, "3 GHz, fundamentally mode-locked, femtosecond Yb-fiber laser," Opt. Lett. **37**(17), 3522–3524 (2012).
27. C. Li, Y. Ma, X. Gao, F. Niu, T. Jiang, A. Wang, and Z. Zhang, "1 GHz repetition rate femtosecond Yb:fiber laser for direct generation of carrier-envelope offset frequency," Appl. Opt. **54**(28), 8350–8353 (2015).
28. Y. Zhou, W. Lin, H. Cheng, W. Wang, T. Qiao, Q. Qian, S. Xu, and Z. Yang, "Composite filtering effect in a SESAM mode-locked fiber laser with a 3.2-GHz fundamental repetition rate: switchable states from single soliton to pulse bunch," Opt. Express **26**(8), 10842–10857 (2018).
29. H. Cheng, W. Wang, Y. Zhou, T. Qiao, W. Lin, S. Xu, and Z. Yang, "5 GHz fundamental repetition rate, wavelength tunable, all-fiber passively mode-locked Yb-fiber laser," Opt. Express **25**(22), 27646–27651 (2017).
30. H. Cheng, W. Wang, Y. Zhou, T. Qiao, W. Lin, S. Xu, and Z. Yang, "Investigation of rectangular shaped wave packet dynamics in a high-repetition-rate ultrafast fiber laser," Opt. Express **25**(17), 20125–20132 (2017).
31. A. Martinez and S. Yamashita, "10 GHz fundamental mode fiber laser using a graphene saturable absorber," Appl. Phys. Lett. **101**(4), 041118 (2012).
32. A. Martinez and S. Yamashita, "Multi-gigahertz repetition rate passively modelocked fiber lasers using carbon nanotubes," Opt. Express **19**(7), 6155–6163 (2011).
33. H. Cheng, W. Lin, Z. Luo, and Z. Yang, "Passively Mode-Locked Tm^{3+}-Doped Fiber Laser With Gigahertz Fundamental Repetition Rate," IEEE J. Sel. Top. Quantum Electron. **24**(1), 1100106 (2018).
34. R. Thapa, D. Nguyen, J. Zong, and A. Chavez-Pirson, "All-fiber fundamentally mode-locked 12 GHz laser oscillator based on an Er/Yb-doped phosphate glass fiber," Opt. Lett. **39**(6), 1418–1421 (2014).

Optics EXPRESS

35. Y. W. Lee, S. Sinha, M. J. F. Digonnet, R. L. Byer, and S. Jiang, "20 W single-mode Yb^{3+} -doped phosphate fiber laser," Opt. Lett. **31**(22), 3255–3257 (2006).
36. Z. C. Luo, M. Liu, H. Liu, X. W. Zheng, A. P. Luo, C. J. Zhao, H. Zhang, S. C. Wen, and W. C. Xu, "2 GHz passively harmonic mode-locked fiber laser by a microfiber-based topological insulator saturable absorber," Opt. Lett. **38**(24), 5212–5215 (2013).
37. A. B. Grudinin, D. J. Richardson, and D. N. Payne, "Passive harmonic mode-locking of a fiber soliton ring laser," Electron. Lett. **29**(21), 1860–1861 (1993).
38. Y. Wang, J. Li, K. Mo, Y. Wang, F. Liu, and Y. Liu, "14.5 GHz passive harmonic mode-locking in a dispersion compensated Tm-doped fiber laser," Sci. Rep. **7**(1), 7779 (2017).
39. X. Liu, T. Wang, C. Shu, L. Wang, A. Lin, K. Lu, T. Zhang, and W. Zhao, "Passively harmonic mode-locked erbium-doped fiber soliton laser with a nonlinear polarization rotation," Laser Phys. **18**(11), 1357–1361 (2008).
40. X. Liu, "Soliton formation and evolution in passively-mode-locked lasers with ultralong anomalous-dispersion fibers," Phys. Rev. A **84**(2), 023835 (2011).
41. A. Chong, W. H. Renninger, and F. W. Wise, "Properties of normal-dispersion femtosecond fiber lasers," J. Opt. Soc. Am. B **25**(2), 140–148 (2008).
42. H. Zhang, D. Y. Tang, L. M. Zhao, X. Wu, and H. Y. Tam, "Dissipative vector solitons in a dispersionmanaged cavity fiber laser with net positive cavity dispersion," Opt. Express **17**(2), 455–460 (2009).
43. H. H. Liu and K. K. Chow, "Enhanced stability of dispersion-managed mode-locked fiber lasers with near-zero net cavity dispersion by high-contrast saturable absorbers," Opt. Lett. **39**(1), 150–153 (2014).
44. F. O. Ilday, J. R. Buckley, W. G. Clark, and F. W. Wise, "Self-similar evolution of parabolic pulses in a laser," Phys. Rev. Lett. **92**(21), 213902 (2004).
45. K. Tamura and M. Nakazawa, "Pulse compression by nonlinear pulse evolution with reduced optical wave breaking in erbium-doped fiber amplifiers," Opt. Lett. **21**(1), 68–70 (1996).
46. R. I. Woodward, "Dispersion engineering of mode-locked fibre lasers," J. Opt. **20**(3), 033002 (2018).
47. W. Chang, A. Ankiewicz, J. M. Soto-Crespo, and N. Akhmediev, "Dissipative soliton resonances in laser models with parameter management," J. Opt. Soc. Am. B **25**(12), 1972–1977 (2008).
48. J. Jeon, J. Lee, and J. H. Lee, "Numerical study on the minimum modulation depth of a saturable absorber for stable fiber laser mode locking," J. Opt. Soc. Am. A **32**(1), 31–37 (2015).
49. T. Schreiber, B. Ortaç, J. Limpert, and A. Tünnermann, "On the study of pulse evolution in ultra-short pulse mode-locked fiber lasers by numerical simulations," Opt. Express **15**(13), 8252–8262 (2007).
50. X. Liu, "Numerical and experimental investigation of dissipative solitons in passively mode-locked fiber lasers with large net-normal-dispersion and high nonlinearity," Opt. Express **17**(25), 22401–22416 (2009).
51. C. Lecaplain, M. Baumgartl, T. Schreiber, and A. Hideur, "On the mode-locking mechanism of a dissipative-soliton fiber oscillator," Opt. Express **19**(27), 26742–26751 (2011).
52. H. Kotb, M. Abdelalim, and H. Anis, "Generalized Analytical Model for Dissipative Soliton in All-Normal-Dispersion Mode-Locked Fiber Laser," IEEE J. Sel. Top. Quantum Electron. **22**(2), 1100209 (2016).
53. D. Y. Tang, L. M. Zhao, B. Zhao, and A. Q. Liu, "Mechanism of multisoliton formation and soliton energy quantization in passively mode-locked fiber lasers," Phys. Rev. A **72**(4), 043816 (2005).
54. A. Haboucha, A. Komarov, H. Leblond, F. Sanchez, and G. Martel, "Mechanism of multiple pulse formation in the normal dispersion regime of passively mode-locked fiber ring lasers," Opt. Fiber Technol. **14**(4), 262–267 (2008).
55. J. M. Soto-Crespo, M. Grapinet, P. Grelu, and N. Akhmediev, "Bifurcations and multiple-period soliton pulsations in a passively mode-locked fiber laser," Phys. Rev. E Stat. Nonlin. Soft Matter Phys. **70**(6), 066612 (2004).
56. N. Akhmediev, J. M. Soto-Crespo, and G. Town, "Pulsating solitons, chaotic solitons, period doubling, and pulse coexistence in mode-locked lasers: complex Ginzburg-Landau equation approach," Phys. Rev. E Stat. Nonlin. Soft Matter Phys. **63**(5), 056602 (2001).
57. H. Cheng, W. Lin, T. Qiao, S. Xu, and Z. Yang, "Theoretical and experimental analysis of instability of continuous wave mode locking: Towards high fundamental repetition rate in Tm3+-doped fiber lasers," Opt. Express **24**(26), 29882–29895 (2016).
58. X. M. Liu, "Interaction and motion of solitons in passively- mode-locked fiber lasers," Phys. Rev. A **84**(5), 053828 (2011).
59. D. Y. Tang, H. Zhang, L. M. Zhao, and X. Wu, "Observation of high-order polarization-locked vector solitons in a fiber laser," Phys. Rev. Lett. **101**(15), 153904 (2008).
60. G. P. Agrawal, *Nonlinear Fiber Optics* (Academic, 2001).
61. O. Shtyrina, M. Fedoruk, S. Turitsyn, R. Herda, and O. Okhotnikov, "Evolution and stability of pulse regimes in SESAM-mode-locked femtosecond fiber lasers," J. Opt. Soc. Am. B **26**(2), 346–352 (2009).
62. F. X. Kartner, J. A. D. Au, and U. Keller, "Mode-locking with slow and fast saturable absorbers - What's the difference? ," IEEE J. Sel. Top. Quantum Electron. **4**(2), 159–168 (1998).